

N. J. Karberg · K. S. Pregitzer · J. S. King
A. L. Friend · J. R. Wood

Soil carbon dioxide partial pressure and dissolved inorganic carbonate chemistry under elevated carbon dioxide and ozone

Received: 4 March 2004 / Accepted: 29 June 2004 / Published online: 16 September 2004
© Springer-Verlag 2004

Abstract Global emissions of atmospheric CO₂ and tropospheric O₃ are rising and expected to impact large areas of the Earth's forests. While CO₂ stimulates net primary production, O₃ reduces photosynthesis, altering plant C allocation and reducing ecosystem C storage. The effects of multiple air pollutants can alter below-ground C allocation, leading to changes in the partial pressure of CO₂ (*p*CO₂) in the soil, chemistry of dissolved inorganic carbonate (DIC) and the rate of mineral weathering. As this system represents a linkage between the long- and short-term C cycles and sequestration of atmospheric CO₂, changes in atmospheric chemistry that affect net primary production may alter the fate of C in these ecosystems. To date, little is known about the combined effects of elevated CO₂ and O₃ on the inorganic C cycle in forest systems. Free air CO₂ and O₃ enrichment (FACE) technology was used at the Aspen FACE project in Rhinelander, Wisconsin to understand how elevated atmospheric CO₂ and O₃ interact to alter *p*CO₂ and DIC concentrations in the soil. Ambient and elevated CO₂ levels were 360 ± 16 and 542 ± 81 μl l⁻¹, respectively; ambient and elevated O₃ levels were 33 ± 14 and 49 ± 24 nl l⁻¹, respectively. Measured concentrations of soil CO₂ and calculated concentrations of DIC increased over the growing season by 14 and 22%, respectively, under elevated atmospheric CO₂ and were unaffected by elevated

tropospheric O₃. The increased concentration of DIC altered inorganic carbonate chemistry by increasing system total alkalinity by 210%, likely due to enhanced chemical weathering. The study also demonstrated the close coupling between the seasonal δ¹³C of soil *p*CO₂ and DIC, as a mixing model showed that new atmospheric CO₂ accounted for approximately 90% of the C leaving the system as DIC. This study illustrates the potential of using stable isotopic techniques and FACE technology to examine long- and short-term ecosystem C sequestration.

Keywords Carbon-13 · Carbon sequestration · FACE · Free air carbon dioxide and ozone enrichment · Global carbonate/silicate weathering cycle

Introduction

Physiological effects of elevated atmospheric CO₂ and tropospheric O₃

Global CO₂ emissions have risen consistently from pre-industrial levels of 275 μl l⁻¹ to current levels in excess of 360 μl l⁻¹, with a concentration of 550 μl l⁻¹ predicted by the middle of this century (Houghton et al. 1996). Concurrent with increasing atmospheric CO₂, tropospheric O₃ levels have risen from pre-industrial levels of 10 nl l⁻¹ to current summer daytime O₃ levels of 50–70 nl l⁻¹. Estimates of increases in tropospheric O₃ of 1–2% per year may result in a tripling of O₃ concentrations within the next 30–40 years (Chameides et al. 1994; Marengo et al. 1994). Even at low concentrations plants exhibit physiological toxicity to O₃ (Karnosky et al. 1996). With 50% of the world's forests expected to experience increased exposure to both CO₂ and O₃ by 2100 (Fowler et al. 1999), the resulting balance of stimulatory/inhibitory effects on physiological processes may profoundly influence the C stocks of terrestrial ecosystems.

N. J. Karberg (✉) · A. L. Friend
USDA Forest Service, North Central Research Station,
410 MacInnes Drive, Houghton, MI 49931, USA
E-mail: nkarberg@fs.fed.us
Tel.: +1-906-4826303
Fax: +1-906-4826355

N. J. Karberg · K. S. Pregitzer · J. S. King
School of Forest Resources and Environmental Science,
Michigan Technological University,
Houghton, MI 49931, USA

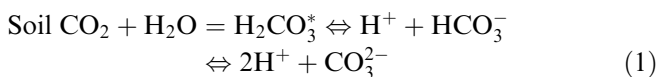
J. R. Wood
Department of Geological and Mining Engineering and Sciences,
Michigan Technological University, Houghton, MI 49931, USA

The interacting effects of these two atmospheric pollutants on ecosystem C dynamics are largely unknown, although their individual effects have been well studied. C3 plant photosynthesis is limited by the concentration of atmospheric CO₂, and an increase in the ratio of CO₂:O₂ will increase C assimilation (Tolbert and Zelitch 1983; Sage 1994). This increase in net photosynthesis under elevated CO₂ has consistently been found to change C cycling in forest ecosystems, including: (1) greater C inputs to soil due to increased rates of litter-fall, root turnover and rhizodeposition (Pregitzer et al. 1995; DeLucia et al. 1999); (2) increased fungal and bacterial activity and enhanced substrate degradation (Phillips et al. 2002); and (3) increased partial pressure of soil CO₂ (soil *p*CO₂) (Andrews and Schlesinger 2001; King et al. 2001).

Whereas CO₂ stimulates photosynthesis, increased tropospheric O₃ reduces photosynthesis compared to ambient concentrations (Reich et al. 1990). The decrease in photosynthesis is caused by oxidative damage to cell membranes, light harvesting processes, C fixation, and disruption of C allocation patterns (Pell 1987; Landry and Pell 1993; Chappelka and Samuelson 1998). Oxidative damage can lead to a number of negative effects on forest productivity that ultimately decrease ecosystem C accumulation. These effects include decreased stomatal conductance and photosynthesis, premature leaf abscission, and decreased leaf size (Coleman et al. 1995). The interactive effects of elevated CO₂ and O₃ have recently been found to strongly influence ecosystem C storage. Loya et al. (2003) found that when forest plots under elevated CO₂ are also exposed to elevated O₃, they formed less new soil C than plots exposed to elevated CO₂ alone. However, virtually nothing is known about how elevated CO₂ and O₃ will interact to affect the inorganic C chemistry of soil solutions in forested ecosystems.

Soil *p*CO₂-dissolved inorganic carbonate interactions

CO₂ and O₃ alter leaf-level plant dynamics, affecting the allocation of photosynthate to root systems, quality of litter inputs, and soil respiration. As CO₂ accumulates in the soil due to the respiration of plant roots and associated soil microorganisms, concentrations of up to 100x atmospheric levels can result (Berthelin 1988). Soil CO₂ reacts with soil water to form dissolved inorganic carbonate (DIC) through the following reaction:



Thus, changes in belowground C allocation driven by leaf-level dynamics can significantly control DIC production.

In our free air CO₂ and O₃ enrichment (FACE) experiment (see below) the application of a two-member

mixing model to DIC chemistry can illustrate the source of increased DIC concentrations in soils. By utilizing the distinct isotopic signal of the highly depleted fumigation CO₂, the measured δ¹³C of soil *p*CO₂, and the measured δ¹³C of DIC, we can show the proportion of DIC-C that is attributable to the fumigation gas. Also, by understanding isotopic fractionation, the seasonal δ¹³C of DIC can be used to provide evidence for altered below-ground chemistry due to changes in soil CO₂ concentrations. Total system DIC, i.e. [DIC], is equal to the summed concentrations of the four inorganic carbonate species:

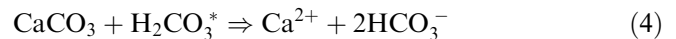
$$[\text{DIC}] = [\text{CO}_{2(\text{aq})}] + [\text{H}_2\text{CO}_3^0] + [\text{HCO}_3^-] + [\text{CO}_3^{2-}] \quad (2)$$

Though by convention, dissolved CO₂ is expressed in its hydrated form as carbonic acid where:

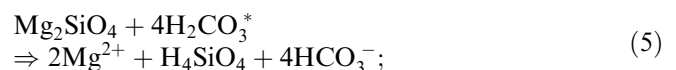
$$[\text{H}_2\text{CO}_3^*] = [\text{H}_2\text{CO}_3^0] + [\text{CO}_{2(\text{aq})}] \quad (3)$$

The speciation of Eq. 2 is determined by soil solution pH. At a soil pH lower than approximately 6.4 (depending upon temperature and soil *p*CO₂), H₂CO₃^{*} dominates DIC, with HCO₃⁻ dominating at pH from 6.4 to 10.3. Significant isotopic fractionation occurs during the pH-mediated speciation of DIC. Soil CO₂ undergoes a 1.1‰ depletion as it forms H₂CO₃^{*}, and then a 9.0‰ enrichment as it forms HCO₃⁻ (Clark and Fritz 1997). Presumably, changes in the δ¹³C ratio of DIC correlate with changes in inorganic chemistry: as soil alkalinity rises, increasing the abundance of HCO₃⁻, the δ¹³C signature of DIC should become increasingly enriched relative to that of soil *p*CO₂.

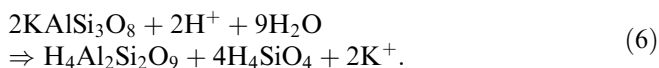
Field studies have shown that elevated atmospheric CO₂ increases the concentration of soil CO₂ (Andrews and Schlesinger 2001; King et al. 2001). Henry's Law (i.e., the amount of gas that dissolves in a liquid is proportional to the partial pressure of the gas over the liquid) dictates that an increase in CO₂ concentration alone will increase the equilibrium concentration of H₂CO₃^{*} by a factor of 10^{-1.5} (Pankow 1991). Thus, not only does elevated soil *p*CO₂ potentially increase the rate of mineral weathering in soil, it can be expected that elevated atmospheric CO₂ increases the rate of amount of mineral weathering by increasing the formation of H₂CO₃^{*} (Berner 1997; Bormann et al. 1998; Berg and Banwart 2000). H₂CO₃^{*} then readily weathers carbonates to form free Ca²⁺ and HCO₃⁻:



Through this reaction, weathering neutralizes acidic CO₂ that is in the form of H₂CO₃^{*}, and keeps it in solution as HCO₃⁻. Silicate weathering meanwhile, extracts alkalinity from silicate minerals, as exhibited by the weathering of olivine by H₂CO₃^{*}:



and/or the hydrolysis of orthoclase feldspar by H^+ :



The combined processes of weathering, riverine export, and deposition of marine carbonates is a transfer and sequestration of atmospheric CO_2 , representing a long-term negative feedback to global warming (Drever 1994; Lackner 2002). However, the extent to which this feedback mechanism has been fully explored under experimental conditions of elevated atmospheric CO_2 is limited and confounded by gaps in understanding the ecosystem-level effects of elevated atmospheric O_3 .

Objectives and hypothesis

The objectives of this study were to determine the effects of elevated CO_2 and O_3 on DIC and soil inorganic chemistry in north temperate forest ecosystems, and comment upon their role in the silicate weathering cycle in soil. This was done by quantifying DIC, tracking the $\delta^{13}C$ signature of the ecosystem, and examining DIC speciation and $\delta^{13}C$ fractionation. Our first hypothesis was that elevated atmospheric CO_2 increases soil pCO_2 and DIC concentrations, while elevated O_3 results in a decrease in soil pCO_2 and DIC. We further hypothesized that soil pH would decrease under elevated CO_2 due to an increase in the activity of H^+ and $H_2CO_3^*$.

Materials and methods

Study site

This study was conducted at the 32-ha FACTS-II Aspen FACE Project, a CO_2 and O_3 enrichment experiment located near Rhinelander, Wisconsin (latitude 45.6°, longitude 89.5°). The soil is a Pandus sandy loam (mixed, frigid, coarse loamy Alfic Haplorthod) derived from non-calcareous sandy to loamy glacial till. These soils were deposited over lower Proterozoic system mafic to felsic and tonalitic to granodioritic rocks. The field experiment consists of a randomized complete block design: three blocks of four treatments (control, elevated CO_2 , elevated O_3 , and elevated $CO_2 + O_3$). The experimental rings are 30 m in diameter and each treatment is replicated 3 times. The rings were planted in June 1997 with trees at a 1×1 m spacing: half of the ring was planted with *Populus tremuloides* var. Michaux (trembling aspen) clones of differing sensitivity to CO_2 and O_3 , a quarter was planted with a 1:1 mix of *P. tremuloides* and *Betula papyrifera* var. Marsh (paper birch), and the final quarter was planted with a mix of *P. tremuloides* and *A. saccharum* var. Marsh (sugar maple). Only the aspen and aspen-birch sections of the ring were measured in this study.

CO_2 is stored and transferred to ambient-air heat exchangers that vaporize the liquefied CO_2 before it is routed as a gas to individual rings. Liquefied O_2 is transferred as needed to an ozone generator before it is routed as O_3 to each ring. At each ring, pipes spaced uniformly around each plot release the fumigation gases in proportions dictated by real-time computer algorithms. For the 2002 growing season the CO_2 fumigation period lasted from 28 May to 11 October for an exposure period of 138 days. Ambient CO_2 levels averaged $360 \pm 16 \mu l l^{-1}$ while the concentration of elevated CO_2 plots averaged $542 \pm 81 \mu l l^{-1}$ (J. Sober, personal communication). The O_3 fumigation period lasted from 29 May to 11 October for an exposure period of 137 days. Ambient O_3 levels averaged $33 \pm 14 \text{ nl } l^{-1}$ while the concentration of elevated O_3 plots averaged $49 \pm 24 \text{ nl } l^{-1}$ (J. Sober, personal communication). A complete description of the project design, justification, hardware, and performance data can be found in Dickson et al. (2000).

Field sampling

Bi-weekly samples were collected from 1 May to 28 October 2002 using belowground collection equipment installed in 1998 and methodology as described by King et al. (2001). Soil pCO_2 was withdrawn from soil gas wells at depths of 15, 30, and 125 cm in each species section and injected into serum vials sealed with butyl rubber septa. Samples were analyzed at the USDA Forestry Sciences Laboratory (Houghton, Mich.) with a Varian CP-3800 gas chromatograph equipped with a thermal conductivity detector; certified NIST-traceable gas was used to develop standard curves. Soil solution was collected using tension lysimeters installed adjacent to each soil gas well. Soil solution was withdrawn, and volume, temperature, pH, and conductivity were measured using a portable pH meter. Water samples were collected in acid-washed HDPE bottles and transported under refrigeration to the laboratory where they were acidified to $pH \approx 2.0$ with HCl, filtered (0.45 μm), and stored at 4°C. The speciation and concentration of DIC was calculated for each sampling date according to well-established carbonate equilibria reactions (Garrels and Christ 1965) using field measured soil pCO_2 , solution pH, and temperature. Field measured pH was corrected for degassing following the method of Suarez (1987) and used to calculate DIC.

The $\delta^{13}C$ of the CO_2 in the fumigation tank was sampled by withdrawing a 50-ml sample from the supply line with a syringe, flushing a 10-ml Exetainer vial (Labco no. 438B) with 40 ml of the gas, and then injecting the final 10 ml. The vial was then subsampled and diluted with He prior to isotopic analysis. Soil pCO_2 for $\delta^{13}C$ analysis was subsampled concurrently with soil pCO_2 . A set of 10-ml Exetainer vials (Labco no. 438B) that had been previously flushed with high purity He was brought into the field. Immediately before sampling,

4 ml He was withdrawn with a syringe from the vial, and 4 ml soil CO₂ for δ¹³C analysis was injected to maintain a constant pressure. DIC for δ¹³C analysis was sampled from lysimeters using a modified gas evolution technique (Atekwana and Krishnamurthy 1998; Andrews and Schlesinger 2001). Using this technique, 0.25 µl of 85% phosphoric acid was added to a Labco Exetainer vial (no. 738 W) that was subsequently evacuated. Immediately upon removal of water from the tension lysimeter, 1.5 ml of the soil solution was injected into the sealed Exetainer vial with a syringe for the δ¹³C analysis of DIC. All samples were analyzed within the 9-day precision estimates provided by Tu et al. (2001). The δ¹³C analyses were performed at the Forest Ecology Stable Isotope Ratio Mass Spectrometry Laboratory in the School of Forest Resources and Environmental Science at Michigan Technological University.

C stable isotope analysis and stable C tracer

The gas isotopic analysis was performed using a ThermoFinnigan GasBench II coupled to a DELTA^{plus} continuous flow-stable isotope ratio mass spectrometer (Bremen, Germany). IAEA-, USGS-, and NIST-certified isotopic standards were used to calibrate standard gas with a δ¹³C value of -49.6‰, relative to V-PDB dolomite, where δ is defined as [(ratio_{sample}/ratio_{standard})-1]×1,000. Overall analytical precision was ±0.3‰ for δ¹³C. The proportion of C in DIC attributable to biogenic pCO₂ (*f*_{bio}) was calculated using the equation: $f_{\text{bio}} = (\delta_1 - \delta_o) / (\delta_2 - \delta_o)$, where δ₁ and δ₂ are the measured δ¹³C values of DIC and soil pCO₂, respectively, and δ_o the δ¹³C value of soil carbonate. The δ¹³C value of soil carbonate was assumed to be -1.7‰, halfway between the reported range of -5.3 to +1.9 as reported by Middleton et al. (1990) for southern Ontario and Taylor and Sibley (1986) for the Michigan basin, respectively. A sensitivity analysis revealed that the range of values had no impact on the results of the mixing model (results not shown). The δ¹³C values of H₂CO₃^{*} and HCO₃⁻ were calculated from fractionation measurements provided by Clark and Fritz (1997). The experimental fumigation CO₂ is derived from fossil fuel and had a cumulative 4-year δ¹³C mean (SD) of -42.1‰ (1.85) from 1999 to 2002. The treatment-level δ¹³C of atmospheric CO₂ means (SD) in the forest canopy in 2002 were: control, -7.6‰ (0.46); +CO₂, -18.5‰ (0.94); +O₃, -7.2‰ (0.22); +CO₂×O₃, -19.0‰ (2.25). These values represent the δ¹³C of atmospheric CO₂ after the fumigation gas was mixed with the ambient atmosphere.

Statistical analysis

Analysis required repeated measures ANOVA since the same experimental units were measured repeatedly over time. Data were analyzed with a repeated measures

ANOVA model for a randomized complete block design using SAS 8.02 (Cary, N.C.) after King et al. (2001). Experimental block is a fixed effect (Dickson et al. 2000) accounting for soil differences across the site. To control for heterogeneity of variance, soil pCO₂, total alkalinity, [DIC], [H₂CO₃^{*}], [HCO₃⁻], [CO₃²⁻], [OH⁻] and [H⁺] normal probability plots were inspected. Data were square root transformed prior to analysis, as this transformation best satisfied model assumptions. Hypothesis tests were conducted at the *P* ≤ 0.05 level of confidence, and trends were reported when *P* < 0.10. Displayed values represent the plot means averaged across the two species split plots (aspen and aspen-birch), three depths (15, 30, and 125 cm), and *n* = 3 replicates. To simplify display, the +O₃ and control treatments and the +CO₂ and +CO₂×O₃ treatments were combined in Figs. 1 and 2. The tabular data remain unchanged.

Results

Soil pCO₂

CO₂ concentrations in the soil atmosphere were positively related to changes in soil temperature. Seasonal patterns in soil pCO₂ appeared to be related to increases in mean daytime soil temperature, with peak soil pCO₂ concentrations occurring with peak soil temperature in July and August (Fig. 1). This gave rise to a highly significant seasonal effect (*P* < 0.001). The soil pCO₂ level in the elevated CO₂ treatments was higher on all sampling dates than in the ambient CO₂ treatments, with this difference being marginal from early May until late June, and most pronounced from July to September, when the soils were warmer. Soil pCO₂ concentrations in the ambient CO₂ plots ranged from 7,000 µl l⁻¹ in early May to a peak of 24,000 µl l⁻¹ in mid July. Soil pCO₂ concentrations in the elevated CO₂ plots followed the same temporal pattern with a 7,500 µl l⁻¹ baseline in early May and a mid July peak of 32,500 µl l⁻¹. Exposure to elevated atmospheric CO₂ significantly increased soil pCO₂ concentrations (*P* = 0.0239), though there were no other significant interactions. Although no other interaction was significant, there was a trend in the data toward a +O₃×Time interaction (*P* = 0.0599). This effect, however, did not appear to be distinct from the other treatments (data not shown).

Dissolved inorganic carbonate

DIC concentrations followed very similar patterns to soil pCO₂ across the growing season, giving rise to a highly significant seasonal effect (*P* < 0.001). Soil DIC concentration was greater in the elevated CO₂ treatment on all sampling dates (*P* = 0.0189), and this difference was consistent through the growing season (Fig. 1c).

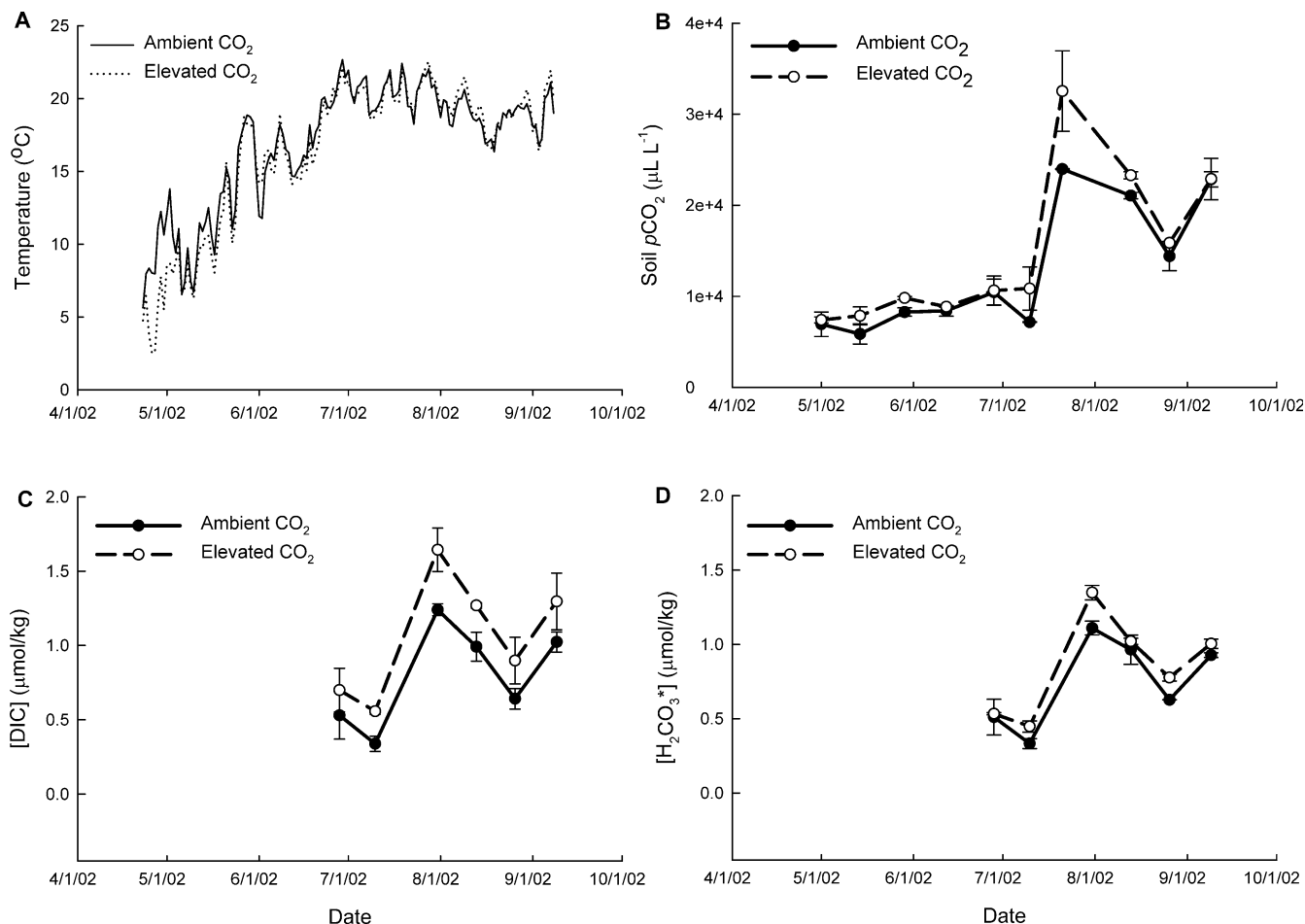


Fig. 1 Seasonal 2002 soil temperature at 10 cm (a), soil partial pressure of CO₂ ($p\text{CO}_2$) (b), soil solution dissolved inorganic carbonate concentration ($[DIC]$) (c), and soil solution carbonic acid concentration ($[H_2CO_3^*]$) (d) at the FACTS II Aspen free air CO₂ and O₃ enrichment (FACE) experiment located near Rhineland, Wisconsin. Ambient and elevated CO₂ levels were 360 ± 16

and $542 \pm 81 \mu\text{L l}^{-1}$, respectively; ambient and elevated O₃ levels were 33 ± 14 and $49 \pm 24 \text{ nl l}^{-1}$, respectively. For display purposes, the +O₃ and control treatments and the +CO₂ and +CO₂×O₃ treatments were combined, respectively. Displayed values are plot means averaged across two species subplots, three depths, and $n = 6$ replicates; bars represent SEs

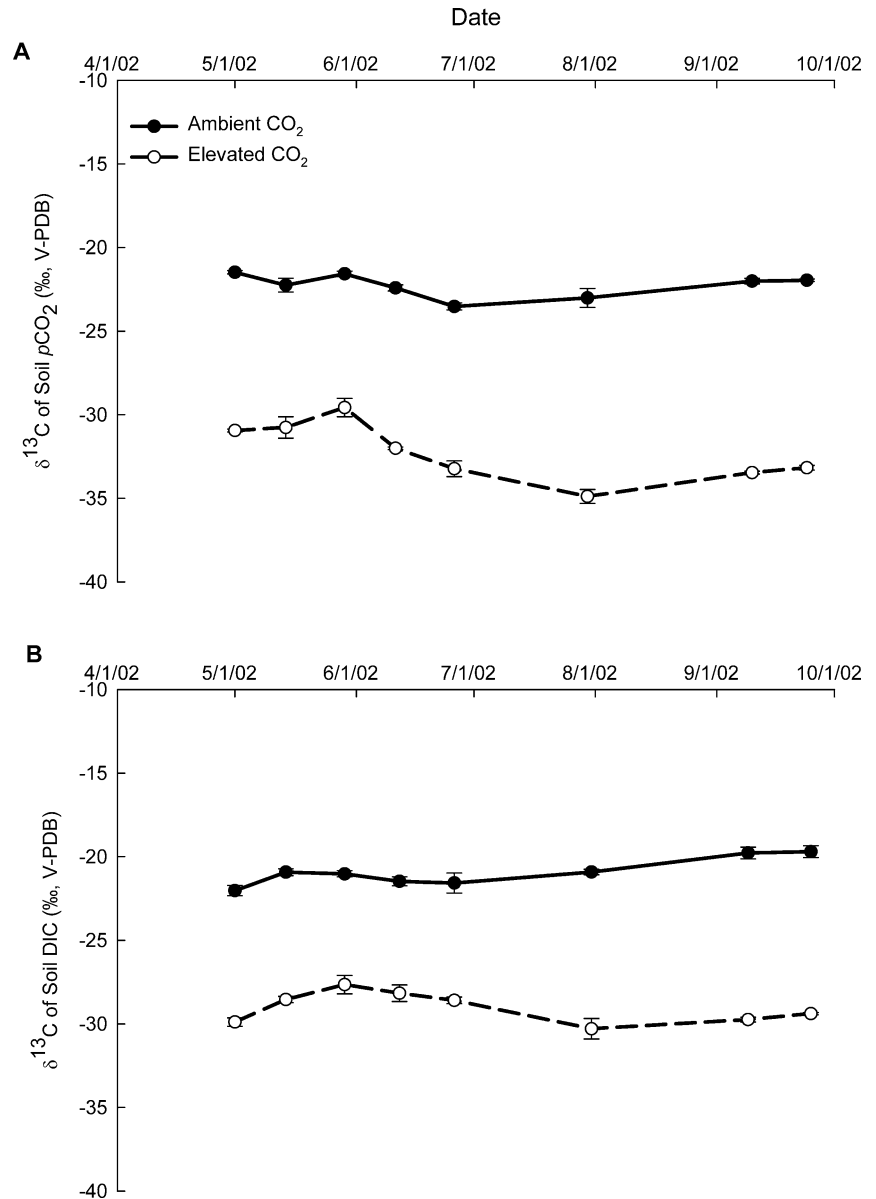
DIC concentrations in the ambient CO₂ plots ranged from 0.33 to $1.24 \mu\text{mol kg}^{-1}$, while concentrations in the elevated CO₂ plots ranged from 0.56 to $1.65 \mu\text{mol kg}^{-1}$. Depth was also significant ($P < 0.001$), with concentrations increasing with increasing soil depth. Although there was a trend in the +CO₂×O₃ treatment towards higher DIC concentrations ($P = 0.0829$) (Table 1); there were no other Species×Time or Species×Depth interactions.

To ensure that the pH correction was not affecting the calculated differences in DIC concentrations, DIC was also calculated using the uncorrected pH measurements. The results were similar to those obtained using the corrected pH (data not shown). Seasonal patterns were very similar to soil $p\text{CO}_2$, with DIC concentrations in the elevated CO₂ treatments consistently higher than those in the ambient treatments ($P = 0.1141$). However, the use of uncorrected pH measurements in the DIC calculation overstated DIC concentrations by 6–24% compared to the use of corrected pH measurements.

Inorganic carbonate chemistry

The concentrations of $H_2CO_3^*$, HCO_3^- , CO_3^{2-} , OH^- and total alkalinity (A_T) followed seasonal patterns similar to that of soil $p\text{CO}_2$ (Fig. 1d, results only shown for $H_2CO_3^*$). Exposure to elevated CO₂ consistently increased ion concentrations and A_T (Table 1). The opposite effect, however, was observed for $[H^+]$, where exposure to elevated CO₂ reduced the concentration. Though these changes were significant for $[H_2CO_3^*]$ ($P = 0.0281$), they were not statistically significant for any other ionic species. All ionic species other than $[H_2CO_3^*]$ exhibited a highly significant depth effect (Table 2): the concentration of $H_2CO_3^*$ and H^+ increased with soil depth, while the concentration of HCO_3^- , CO_3^{2-} , OH^- and A_T decreased with soil depth. Time was also highly significant for A_T and all ionic species, except $[H^+]$ and $[OH^-]$, with peak concentrations occurring in August. These results were driven by changes in soil $p\text{CO}_2$ with depth, time of year, and treatment.

Fig. 2 Seasonal 2002 $\delta^{13}\text{C}$ of soil $p\text{CO}_2$ (a) and DIC (b) at the FACTS II Aspen FACE experiment. Ambient and elevated CO_2 levels were 360 ± 16 and $542 \pm 81 \mu\text{l l}^{-1}$, respectively; ambient and elevated O_3 levels were 33 and $49 \pm 24 \text{ nl l}^{-1}$, respectively. For display purposes, the $+\text{O}_3$ and control treatments and the $+\text{CO}_2$ and $+\text{CO}_2 \times \text{O}_3$ treatments have been combined, respectively. Displayed values are plot means averaged across two species subplots, three depths, and $n = 6$ replicates; bars represent SEs. For abbreviations, see Fig. 1



$\delta^{13}\text{C}$ of soil $p\text{CO}_2$

The heavily depleted $\delta^{13}\text{C}$ signal of the fumigation gas led to significant ($P < 0.001$) differences in the isotopic ratio of soil $p\text{CO}_2$ between the ambient and elevated CO_2 treatments (Table 3). The average $\delta^{13}\text{C}$ of soil $p\text{CO}_2$ values in ambient CO_2 plots was measured at -21.5‰ in May, and became steadily more depleted to -23.5‰ in early July (Fig. 2a). Values then became steadily enriched into October. The $\delta^{13}\text{C}$ of soil $p\text{CO}_2$ followed a different pattern in the elevated CO_2 treatment. $\delta^{13}\text{C}$ values were measured at -30.0‰ in May, and became consistently depleted to values of -34.9‰ in late July. Values then became slightly enriched into October. Though values in the elevated atmospheric CO_2 treatments were already depleted by 9.0‰ , they became increasingly depleted relative to ambient CO_2 treatments as the growing season progressed. These

patterns gave rise to a significant seasonal time effect ($P < 0.001$) and $+\text{CO}_2 \times \text{Time}$ effect ($P < 0.001$). A strong species effect was observed, with the $\delta^{13}\text{C}$ of soil $p\text{CO}_2$ becoming more depleted in aspen-birch subplots than in pure aspen subplots ($P = 0.0058$) (data not shown). A strong depth effect was also observed, with $\delta^{13}\text{C}$ values becoming more depleted with depth in the soil profile ($P = 0.0086$) (data not shown). The $\delta^{13}\text{C}$ of the fumigation gas was consistent throughout the growing season and did not explain the isotopic variation seen in the CO_2 fumigated plots.

$\delta^{13}\text{C}$ of DIC

The depleted $\delta^{13}\text{C}$ signal in the fumigation gas also led to significant differences in isotopic ratios between ambient and elevated CO_2 plots for DIC ($P < 0.001$),

Table 1 Inorganic C species concentrations at the FACTS II Aspen free air CO₂ and O₃ enrichment (FACE) experiment^a located near Rhinelander, Wisconsin. Displayed values are plot means averaged across two species subplots, three depths, six sampling dates, and $n = 3$ replicates with the SE given in parentheses. Different letters following means represent significantly different values by treatment (repeated measures ANOVA, $\alpha = 0.05$). $p\text{CO}_2$ Partial pressure of CO₂, DIC dissolved inorganic carbonate, A_T Total alkalinity

Treatment	Soil $p\text{CO}_2$ ($\mu\text{l l}^{-1}$) ^b	DIC ($\mu\text{mol/kg}$)	H ₂ CO ₃ [*] ($\mu\text{mol/kg}$)	HCO ₃ ⁻ ($\mu\text{mol/kg}$)	H ⁺ (nmol/kg)	CO ₃ ²⁻ (pmol/kg)	OH ⁻ (pmol/kg)	A_T ($\mu\text{mol/kg}$) ^c
Control	13,500 (890) a	0.84 (0.06) a	0.75 (0.05) a	0.09 (0.02) a	23.3 (4.61) a	2.66 (0.96) a	2.76 (0.37) a	0.07 (0.02) a
+CO ₂	14,700 (800) b	0.98 (0.07) b	0.84 (0.06) b	0.14 (0.03) a	16.1 (6.05) a	7.00 (3.24) a	4.82 (0.92) a	0.13 (0.03) a
+O ₃	13,100 (810) a	0.83 (0.05) a	0.73 (0.05) a	0.10 (0.03) a	216.8 (118.5) a	2.41 (0.38) a	3.57 (0.37) a	-0.11 (0.12) a
+CO ₂ ×O ₃	15,700 (900) b	1.06 (0.06) b	0.86 (0.05) b	0.20 (0.03) a	18.2 (3.79) a	12.98 (3.76) a	5.64 (1.00) a	0.18 (0.03) a

^aAmbient and elevated CO₂ levels were 360 ± 16 and $542 \pm 81 \mu\text{l l}^{-1}$, respectively; ambient and elevated O₃ levels were 33 ± 14 and $49 \pm 24 \text{ nl l}^{-1}$. Soil $p\text{CO}_2$ was directly measured; DIC, A_T , and speciation were calculated from measured soil $p\text{CO}_2$, temperature, and pH according to carbonate equilibria reactions formulated by Garrels and Christ (1965)

though no differences were seen for elevated O₃, $\delta^{13}\text{C}$ of DIC in ambient CO₂ plots was measured at -22.0‰ in May, and became consistently enriched to values of -19.7‰ in October (Fig. 2b). $\delta^{13}\text{C}$ values followed a different pattern in the elevated CO₂ treatment, which also could not be explained by the seasonal $\delta^{13}\text{C}$ of the fumigation gas. $\delta^{13}\text{C}$ values were measured at -29.0‰ in early May, and became enriched to a value of -27.6‰ in late May (Fig. 2b). Values then became consistently depleted to -30.0‰ in October. This gave rise to a highly significant time effect ($P < 0.001$). While $\delta^{13}\text{C}$ values in elevated CO₂ treatments became more depleted relative to those in the ambient CO₂ plots, there were no significant time interactions to explain this tendency. No Species, Species×Time, Depth, or Species×Depth interactions were significant. As $\delta^{13}\text{C}$ of H₂CO₃ and HCO₃⁻ were calculated from $\delta^{13}\text{C}$ of soil $p\text{CO}_2$, these trends follow those of soil $p\text{CO}_2$ and thus P -values are not displayed, although annual means are displayed in Table 3.

Discussion

Elevated atmospheric CO₂ has been hypothesized to increase soil $p\text{CO}_2$ through increased fine root production and turnover, and resulting increases in the respiration of autotrophs (R_A) and heterotrophs (R_H). Fine root production (measured in 1999) in the same stands of *P. tremuloides* increased 96% relative to the control under experimental atmospheric CO₂ enrichment (King et al. 2001). *P. tremuloides* fine root biomass was also shown to increase by 52% under elevated atmospheric CO₂ in an open top chamber study (Pregitzer et al. 2000). An increase in fine root biomass of 86% has also been reported for a similar forested FACE experiment of *Pinus taeda* (Matamala and Schlesinger 2000). While these increases in fine root standing stock represent increased levels of R_A , they also facilitate increases in R_H . For the 1999 data, King et al. (2001) reported a 139% increase in dead-root stock under elevated CO₂, and the authors have concluded that elevated atmospheric CO₂ increases fine root turnover (Kubiske et al. 1998; Pregitzer et al. 1995, 2000). As most microbial communities are C limited (Zak and Pregitzer 1998), this enhanced addition of organic matter through organic acids, root turnover, and increased microbial metabolism likely increased R_H as well (Zak et al. 2000).

Soil $p\text{CO}_2$ concentrations, averaged across soil depths and species subplots increased by 14% under elevated CO₂. Similar increases under elevated CO₂ have previously been reported (Andrews and Schlesinger 2001; King et al. 2001). With increasing concentrations of soil CO₂, Eq. 1 is driven to the right, increasing the production of DIC. The increase in DIC was calculated to be 22% under elevated CO₂. Though DIC concentrations were calculated with pH values that were corrected for tension lysimeter degassing, it is noted that DIC

Table 2 *P*-values for calculated carbonate chemistry speciation at the FACTS II Aspen FACE experiment^a. Appropriate *F*-test error terms for a split-plot randomized design with a fixed block effect. Significant ($\alpha=0.05$) values are shown as well as trends ($\alpha < 0.10$)

Source	[H ₂ CO ₃]	[HCO ₃ ⁻]	[H ⁺]	[CO ₃ ²⁻]	[OH ⁻]	A _T
+ CO ₂	0.0281					
+ CO ₂ ×O ₃ ×Species	0.0829					
Time	< 0.001	0.0026		0.0160	0.0796	0.0002
+ O ₃ ×Time	0.0957					
+ CO ₂ ×Species×Time	0.0325					
+ O ₃ ×Species×Time					0.0593	
Depth		0.0010	0.0029	0.0005	0.0006	0.0001
+ O ₃ ×Depth						0.0451

^aAmbient and elevated CO₂ levels were 360 ± 16 and 542 ± 81 μl l⁻¹, respectively; ambient and elevated O₃ levels were 33 ± 14 and 49 ± 24 nl l⁻¹, respectively

Table 3 A comparison of δ¹³C ratios from the FACTS II Aspen FACE experiment^a. Displayed values are plot means averaged across two species subplots, three depths, eight sampling dates, and *n* = 3 replicates with the SE given in parentheses. Different letters

following column means represent significantly different values by treatment (repeated measures ANOVA, $\alpha=0.05$). For abbreviations, see Table 1

Treatment	δ ¹³ pCO ₂ (‰) ^b	δ ¹³ DIC (‰) ^b	δ ¹³ H ₂ CO ₃ (‰) ^c	δ ¹³ HCO ₃ (‰) ^c	pCO ₂ -C as DIC-C (‰) ^d
Control	-21.5 (0.29) a	-21.6 (0.12) a	-22.6 (0.30) a	-13.6 (0.30) a	100.0 (0.67)
+ CO ₂	-32.4 (0.31) b	-29.6 (0.26) b	-33.5 (0.31) b	-24.5 (0.31) b	92.3 (0.01)
+ O ₃	-20.7 (1.05) a	-20.5 (0.13) a	-21.8 (1.05) a	-12.8 (1.05) a	99.2 (3.70)
+ CO ₂ ×O ₃	-32.3 (0.31) b	-28.8 (0.26) b	-33.4 (0.31) b	-24.4 (0.31) b	90.4 (0.06)

^aAmbient and elevated CO₂ levels were 360 ± 16 and 542 ± 81 μl l⁻¹, respectively; ambient and elevated O₃ levels were 33 ± 14 and 49 ± 24 nl l⁻¹, respectively

^dThe percentage of DIC-C derived from soil pCO₂ was calculated using a mixing model (see Materials and methods)

^bδ¹³pCO₂ and δ¹³ DIC were directly measured

^cδ¹³ H₂CO₃ and δ¹³ HCO₃ were calculated from measured δ¹³pCO₂ and fractionation measurements provided by Clark and Fritz (1997) and Zhang et al. (1994)

calculations utilizing uncorrected pH measurements may overstate DIC concentrations by up to 25%, since the concentration of DIC increases with pH (Fig. 3). The concentration of H₂CO₃^{*} increased by 22% due to increased concentrations of soil CO₂, as governed by the Henry's law constant, *K_H*. However, while the concentration of H₂CO₃^{*} increased under elevated CO₂, it made up a proportionately smaller percentage of DIC-C. The percentage of DIC-C existing as HCO₃⁻ increased from 11% under ambient CO₂ to 17% under elevated CO₂. This proportional increase in HCO₃⁻ under elevated CO₂ is accompanied by increases in the concentrations of carbonate (CO₃²⁻), hydroxide (OH⁻), and total alkalinity, as well as a decrease in the concentration of H⁺.

Taken together these results support our first hypothesis that elevated atmospheric CO₂ can be shown to increase soil pCO₂ and concentrations of DIC. Trends in the data also suggest support for our hypothesis that elevated O₃ reduces soil pCO₂ and DIC. The effects of elevated O₃, however, are not statistically distinguishable from the other treatments. These data do not support our second hypothesis, that soil acidity will increase under elevated CO₂ due to increased concentrations of H⁺ and H₂CO₃^{*}. The data instead show the opposite effect, that elevated atmospheric CO₂

increases soil alkalinity, and that soil pH is buffered by changes in soil inorganic carbonate chemistry under elevated CO₂. These observations are explained by an open system model of equilibrium carbonate chemistry (Fig. 3).

In the ambient CO₂ model, the open system equilibrium model is driven by the external soil pCO₂ concentration of 13,500 μl l⁻¹. Through carbonate equilibria equations and Henry's Law, the concentration of external soil pCO₂ then dictates [H₂CO₃^{*}], which remains constant across the pH range. While [H₂CO₃^{*}] remains constant, total DIC increases after pH 5.0 because of the increasing contribution of HCO₃⁻ until the species contribute an equal portion of C to DIC. Under elevated atmospheric CO₂, the system is driven by the external soil pCO₂ concentration of 14,500 μl l⁻¹. This greater concentration of external soil pCO₂ under elevated CO₂ then establishes a greater concentration of H₂CO₃^{*}. Figure 3 illustrates the result of these shifts in the open system equilibrium model. Under elevated soil pCO₂, the concentration of H₂CO₃^{*} increases, as does the concentration of HCO₃⁻. However, due to a small increase in pH the elevated CO₂ system equilibrium point moves to the right as well, explaining the greater proportion of HCO₃⁻-derived C in DIC (Fig. 3).

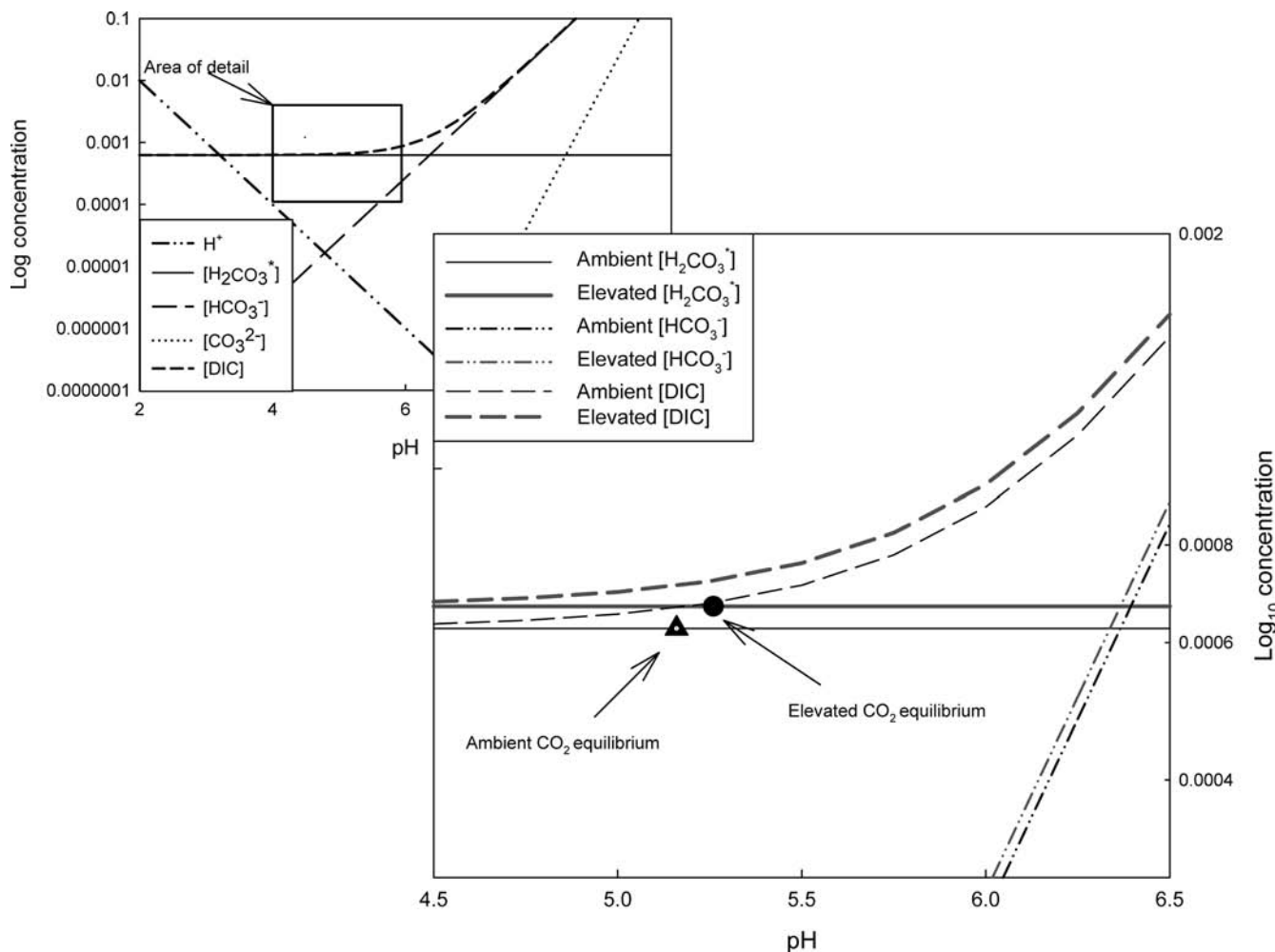


Fig. 3 Open system equilibrium diagram for ambient CO_2 FACE conditions of 16.3°C , pH of 5.16 and soil $p\text{CO}_2$ of $10^{-1.87}$

Seasonal $\delta^{13}\text{C}$ data also support the assumptions of the open system equilibrium model. Distribution models show that system pH governs the distribution of carbonate species in water (Clark and Fritz 1997). In the FACTS II Aspen FACE experiment, H_2CO_3^* is the dominant C-bearing species, with the importance of HCO_3^- increasing with pH. Fractionation models show that this pH-mediated speciation results in a temperature-dependent fractionation, with $\delta^{13}\text{C}$ values becoming depleted by approximately 1.1‰ from $\text{CO}_{2(\text{g})}$ to H_2CO_3^* , and enriched 9.0‰ from H_2CO_3^* to HCO_3^- (Zhang et al. 1994; Clark and Fritz 1997). Thus, with a $\delta^{13}\text{C}$ of soil $p\text{CO}_2$ of -21‰ , DIC having a pure H_2CO_3^* or HCO_3^- source would be -22.2 and -13.2‰ , respectively. Under ambient CO_2 , the $\delta^{13}\text{C}$ of DIC is very similar to soil $p\text{CO}_2$, suggesting very little influence of HCO_3^- on $\delta^{13}\text{C}$. However, under elevated CO_2 , the measured $\delta^{13}\text{C}$ of DIC is enriched compared to soil $p\text{CO}_2$, suggesting a larger contribution of the enriched HCO_3^- to total DIC. It is unlikely that this pattern was complicated by contamination from local carbonate

($13,500 \mu\text{l l}^{-1}$). Ambient and elevated CO_2 levels were 360 ± 16 and $542 \pm 81 \mu\text{l l}^{-1}$, respectively; ambient and elevated O_3 levels were 33 ± 14 and $49 \pm 24 \text{ nl l}^{-1}$, respectively. Inset illustrates equilibrium model shifts under the elevated CO_2 FACE system

minerals with $\delta^{13}\text{C}$ ranges from -5.3 to 1.9‰ as reported by Middleton et al. (1990) for southern Ontario and Taylor and Sibley (1986) for the Michigan basin. Carbonates have already been weathered from the upper meter of this soil (D. R. Zak, personal communication), and laboratory tests for the presence of inorganic carbonate were negative (data not shown). Furthermore, seasonal $\delta^{13}\text{C}$ of soil $p\text{CO}_2$ and DIC showed no influence of enrichment that could be caused by rising water tables or hydraulic lift carrying carbonate-contaminated water from deeper soil to the near surface. Measured $\delta^{13}\text{C}$ of DIC and soil $p\text{CO}_2$ in the elevated CO_2 treatments agrees well with values calculated in the manner of Stumm and Morgan (1981) as displayed in Amiotte-Suchet et al. (1999) and values from another FACE system (Andrews and Schlesinger 2001). Values in the ambient CO_2 treatments also fall within the range of natural variation found in forest ecosystems (Kendall and McDonnell 1998).

Taken together, these data suggest to us that elevated atmospheric CO_2 alters ecosystem inorganic carbonate

chemistry. A 50% increase in atmospheric CO₂ resulted in a 14% increase in soil *p*CO₂ concentrations. In the absence of carbonate, soil *p*CO₂ would account for all C present in DIC (Kendall and McDonnell 1998). With the use of a mixing model and assumed values of soil carbonate (see Materials and methods), 95–100% of DIC–C is attributable to biogenic *p*CO₂, establishing elevated atmospheric CO₂ as the direct cause of increased DIC concentration and altered speciation (Table 3). This finding also provides evidence that short-term terrestrial C cycling may be linked to the long-term silicate C weathering cycle through a time step shorter than may have been previously assumed. Soil *p*CO₂ increased by 14% under elevated CO₂ and [H₂CO₃*] increased by 14% also, as expected by *K_H*. However, calculated DIC concentrations increased by 22%, with a 78% increase in [HCO₃[–]], a 294% increase in [CO₃^{2–}], and a 210% increase in *A_T*. The increases in [DIC] have likely contributed to the calculated increase in speciation and *A_T*. These increases may also be due in part to enhanced primary mineral weathering by increased production of H₂CO₃*. It is possible that weathering of silicates (Eqs. 4, 5) increases alkalinity through the production of HCO₃[–] and OH[–]. Sufficient amounts of P- or S-bearing minerals could result in the weathering of sulfate and phosphate in concentrations high enough to neutralize H⁺, explaining the pattern seen in [H⁺] under elevated CO₂ in Table 3. It is even possible that carbonate minerals such as calcite (Eq. 3) or dolomite could contribute excess inorganic carbonate, though this is unlikely without the presence of soil inorganic carbonate.

Conclusions

This study has shown that elevated atmospheric CO₂ increased soil *p*CO₂, [DIC], and [H₂CO₃*]: the effects of elevated O₃ were transient or muted, and require further study. In addition to increasing concentrations of C in soil solution, the study has shown that elevated atmospheric CO₂ alters system inorganic carbonate chemistry by increasing alkalinity, with the potential to increase weathering rates of primary minerals. Given an estimated annual oceanic DIC input of 0.4×10¹⁵ g C year^{–1} (Schlesinger 1997), and extrapolating a 22% increase in soil solution DIC concentration as reported here to be consistent across soil types throughout the world, we calculate a potential 0.1×10¹⁵ g C year^{–1} increase in global DIC delivery to the ocean, a rate consistent with estimates cited in Houghton (2003). Though DIC is a minor global CO₂ flux compared to net primary production and respiration (60×10¹⁵ g C year^{–1}, Schimel 1995), it represents a potential long-lived sequestration reservoir in deep ocean sediments. This extrapolation is not intended to be a robust parameter for global C modeling; however, it illustrates that aggrading forest ecosystems may be used to capture and sequester atmospheric CO₂ through inorganic processes.

Acknowledgements This study was aided by the help of numerous people: J. Taylor, E. Nauertz, R. Ketterer, W. Loya, M. Porter, R. Peryam, K. Larsen, J. Ashby, J. Eikenberry, and A. Johansen. This research was supported by the US Department of Energy's Office of Science (Program for Ecosystem Research and National Institute for Global Environmental Change), the USDA Forest Service (Northern Global Change Program and North Central Research Station), the National Science Foundation (DEB, DBI/MRI), and the USDA National Research Initiatives Competitive Grants Program. G. Hendrey, K. Lewin, J. Nagey, D. Karnsoky, and J. Sober have been instrumental in the successful implementation of this long-term study.

References

- Amiotte-Suchet P, Aubert D, Probst JL, Gauthier-Lafaye F, Probst A, Andreux F, Viville D (1999) δ¹³C pattern of dissolved inorganic carbon in a small granitic catchment: the (2000) Strengbach case study (Vosges mountains, France). *Chem Geol* 159:129–145
- Andrews JA, Schlesinger WH (2001) Soil CO₂ dynamics, acidification, and chemical weathering in a temperate forest with experimental CO₂ enrichment. *Glob Biogeochem Cycles* 15(1):149–162
- Atekwana EA, Krishnamurthy RV (1998) Seasonal variations of dissolved inorganic carbon and d13C of surface waters: application of a modified gas evolution technique. *J Hydrol* 205:265–278
- Berg A, Banwart SA (2000) Carbon dioxide mediated dissolution of Ca-feldspar: implications for silicate weathering. *Chem Geol* 163:25–42
- Berner RA (1997) The rise of plants and their effect on weathering and atmospheric CO₂. *Science* 276:544–546
- Berthelin J (1988) Microbial weathering processes in natural environments. In: Lerman A, Meybeck M (eds) *Physical and chemical weathering in geochemical cycles*. Kluwer, Dordrecht, pp 33–59
- Bormann BT, Wang D, Bormann FH, Benoit G, April R, Snyder R (1998) Rapid, plant-induced weathering in an aggrading experimental ecosystem. *Biogeochemistry* 43:129–155
- Chameides WL, Kasibhatla PS, Yienger J, Levy H II (1994) Growth of continental-scale, metro-agro-plexes, regional ozone pollution, and world food production. *Science* 264:74–77
- Chappelka AH, Samuelson LJ (1998) Ambient ozone effects on forest trees in the Eastern United States: a review. *New Phytol* 139:91–108
- Clark ID, Fritz P (1997) *Environmental isotopes in hydrogeology*. CRC, New York
- Coleman MD, Isebrands JG, Dickson RE, Karnosky DF (1995) Photosynthetic productivity of aspen clones varying in sensitivity to tropospheric ozone. *Tree Physiol* 15:585–592
- DeLucia EH, Hamilton JG, Naidu SL, Thomas RB, Andrews JA, Finzi A, Lavine M, Matamala R, Mohan JE, Hendrey GR, Schlesinger WH (1999) Net primary production of a forest ecosystem with experimental CO₂ enrichment. *Science* 289:1177–1179
- Dickson RE, Lewin KF, Isebrands JG, Coleman MD, Heilman WE, Riemenschneider DE, Sober J, Host GE, Zak DR, Hendrey GR, Pregitzer KS, Karnosky DF (2000) Forest atmosphere carbon transfer and storage (FACTS-II). The aspen free-air CO₂ and O₃ enrichment (FACE) project: an overview. USDA Forest Service. General Technical Report NC–214
- Drever JI (1994) The effect of land plants on weathering rates of silicate minerals. *Geochim Cosmochim Acta* 58(10):2325–2332
- Fowler D, Cape JN, Coyle M, Flechard C, Kuylenstierna J, Hicks K, Derwent D, Johnson C, Stevenson D (1999) The global exposure of forests to air pollutants. *Water Air Soil Pollut* 116:5–32
- Garrels RM, Christ CL (1965) *Solutions, minerals, and equilibria*. Harper-Collins, New York

- Houghton RA (2003) Why are estimates of the terrestrial carbon balance so different? *Global Change Biol* 9:500–509
- Houghton JT, Meira Filho LG, Callander BA, Harris N, Kattenberg A, Maskell K (1996) *Climate change 1995: the science of climate change* Cambridge University Press, Cambridge
- Karnosky DF, Gagnon ZE, Dickson RE, Coleman MD, Lee EH, Isebrands JG (1996) Changes in leaf growth, leaf abscission, and biomass associated with seasonal tropospheric ozone exposures of *Populus tremuloides* clones and seedlings. *Can J For Res* 26:23–37
- Kendall C, McDonnell JJ (1998) *Isotope tracers in catchment hydrology*. Elsevier, New York
- King JS, Pregitzer KS, Zak DR, Sober J, Isebrands JG, Dickson RE, Hendrey GR, Karnosky DF (2001) Fine-root biomass and fluxes of carbon in young stands of paper birch and trembling aspen as affected by elevated atmospheric CO₂ and tropospheric O₃. *Oecologia* 128:237–250
- Kubiske ME, Pregitzer KS, Zak DR, Mikan CJ (1998) Growth and C allocation of *Populus tremuloides* genotypes in response to atmospheric CO₂ and soil N availability. *New Phytol* 140:251–260
- Lackner KS (2002) Carbonate chemistry for sequestering fossil carbon. *Annu Rev Energy Environ* 27:193–232
- Landry LG, Pell EJ (1993) Modification of Rubisco and altered proteolytic activity in O₃-stressed hybrid poplar (*Populus maximowizii* × *trichocarpa*). *Plant Physiol* 101:1355–1362
- Loya WM, Pregitzer KS, Karberg NJ, King JS, Giardina CP (2003) Reduction of soil carbon formation by tropospheric ozone under increased carbon dioxide levels. *Nature* 425:705–707
- Marenco A, Gouget H, Nedelec P, Pages JP, Karcher F (1994) Evidence of a long-term increase in tropospheric ozone from Pic du Midi series: consequences: positive radiative forcing. *J Geophys Res* 99(D8):16617–16632
- Matamala R, Schlesinger WH (2000) Effects of elevated atmospheric CO₂ on fine root production and activity in a temperate forest ecosystem. *Global Change Biol* 6:967–980
- Middleton K, Coniglio M, Frape SK (1990) Burial dedolomitization, Middle Ordovician carbonates, southwestern Ontario. *AAPG Bull* 74:1308
- Pankow JF (1991) *Aquatic chemistry concepts*. Lewis, Chelsea
- Pell EJ (1987) Ozone toxicity—is there more than one mechanism of action? In: Hutchinson TC, Meema KM (eds) *Effects of atmospheric pollutants on forests, wetlands, and agricultural ecosystems*. (NATO ASI series, vol G16) Springer, Berlin Heidelberg New York, pp 229–240
- Phillips RL, Zak DR, Holmes WE, White DC (2002) Microbial community composition and function beneath temperate trees exposed to elevated atmospheric carbon dioxide and ozone. *Oecologia* 131:236–244
- Pregitzer KS, Zak DR, Curtis PS, Kubiske ME, Teeri JA, Vogel CS (1995) Atmospheric CO₂, soil nitrogen, and turnover of fine roots. *New Phytol* 129:579–585
- Pregitzer KS, Zak DR, Masiarz J, DeForest J, Curtis PS, Lussenhop J (2000) Interactive effects of atmospheric CO₂ and soil-N availability on the fine roots of *Populus tremuloides*. *Ecol Appl* 10:18–33
- Reich PB, Ellsworth DS, Kloeppel BD, Fownes JH, Gower ST (1990) Vertical variation in canopy structure and CO₂ exchange of oak-maple forests influence of ozone, nitrogen, and other factors on simulated canopy carbon gain. *Tree Physiol* 7:329–345
- Sage RF (1994) Acclimation of photosynthesis to increasing atmospheric CO₂: the gas exchange perspective. *Photosynth Res* 39:351–368
- Schimel DS (1995) Terrestrial ecosystems and the carbon cycle. *Global Change Biol* 1:77–91
- Schlesinger WH (1997) *Biogeochemistry: an analysis of global change*. Academic Press, New York
- Stumm W, Morgan JJ (1981) *Aquatic chemistry*. Wiley, New York
- Suarez DL (1987) Prediction of pH errors in soil-water extractors due to degassing. *Soil Sci Soc Am J* 51:64–67
- Taylor TR, Sibley DF (1986) Ferroan dolomite in the Trenton formation, Ordovician Michigan Basin. *Sedimentology* 33:61–86
- Tolbert NE, Zelitch I (1983) Carbon metabolism. In: Lemon ER (eds) *CO₂ in plants*. Westview, Boulder, Colo., pp 71–88
- Tu KP, Brooks PD, Dawson TE (2001) Using septum-capped vials with continuous flow isotope ratio mass spectrometric analysis of atmospheric CO₂ for Keeling plot applications. *Rapid Commun Mass Spectrom* 15
- Zak DR, Pregitzer KS (1998) Integration of ecophysiological and biogeochemical approaches to ecosystem dynamics. In: Pace M, Groffman P (eds) *Successes, limitations, and frontiers in ecosystem science*. Springer, Berlin Heidelberg New York, pp 372–403
- Zak DR, Pregitzer KS, King JS, Holmes WE (2000) Elevated atmospheric CO₂, fine roots and the response of soil microorganisms: a review and hypothesis. *New Phytol* 147:201–222
- Zhang J, Quay PD, Walbur DO (1994) Carbon isotope fractionation during gas-water exchange and dissolution of CO₂. *Geochim Cosmochim Acta* 59:107–114